Growth of tungsten nanoparticles in direct-current argon glow discharges

L. Couëdel, Kishor Kumar K., and C. Arnas

Aix-Marseille Univ./CNRS, Laboratoire PIIM, 13397 Marseille Cedex 20, France.

Abstract

The growth of nanoparticles from the sputtering of a tungsten cathode in DC argon glow discharges is reported. The growth by successive agglomerations is evidenced. The evolution of the discharge voltage, electron density and emission line intensities during particle growth can be divided in four separate phases and exhibit distinctive features. The evolution of the different parameters is explained by a competition between the surface state of the tungsten cathode and the influence of the growing nanoparticles.

Introduction

In this article, we report on the growth of tungsten nanoparticles from the sputtering of a tungsten cathode in a direct-current (DC) argon glow discharge. A detailed study at a fixed argon pressure and discharge current was performed. We show that tungsten nanoparticles are agglomerates of tungsten nanocrystallites. It is also shown that these particles modified the discharge voltage and the emission line intensities of various plasma species, all of which exhibiting strong variations. We provided evidence that the variations of the discharge and plasma parameters during particle growth were strongly dependent on the the nature and the surface state of the cathode material.

Experimental set-up

It is contained in a cylindrical vacuum chamber of 30 cm diameter and 40 cm length. DC glow discharges in argon at a static pressure of 0.6 mbar were initiated between two parallel electrodes: a tungsten cathode of 9.9 cm diameter and a grounded stainless steel anode. The electrodes were separated by a distance of 10 cm by two half glass cylinders. The anode disc had a hole at the centre through which the tungsten nanoparticles produced during the discharge were collected. A regulated power supply was used to bias the cathode. The discharge current density was kept at a constant value (0.53 mA·cm^{-2}). The cathode voltage was $V_d \sim -600$ V giving a total flux of impinging particles $\Phi_t \sim 7 \cdot 10^{15}$ cm^{-2}/s, a sputtering yield was $\Upsilon \sim 3.8$ % and a flux of sputtered tungsten atom $\Phi_W \sim 3 \cdot 10^{14}$ cm^{-2}/s [1]. The chosen discharge parameters were favourable to nanoparticle formation by homogeneous nucleation from the sputtered atoms. OES study of the discharge plasma was carried out. The intensity of different emission

lines - ArI , ArII , WI , WII , H_α - were measured using two monochromators coupled to photomultiplier tubes . The evolution of the electron density was measured using a commercial microwave interferometer operating at 26.5 GHz. The size distributions of the collected dust particles were established using SEM and their structures were analysed by High Resolution - Transmission Electron Microscopy (HR-TEM).

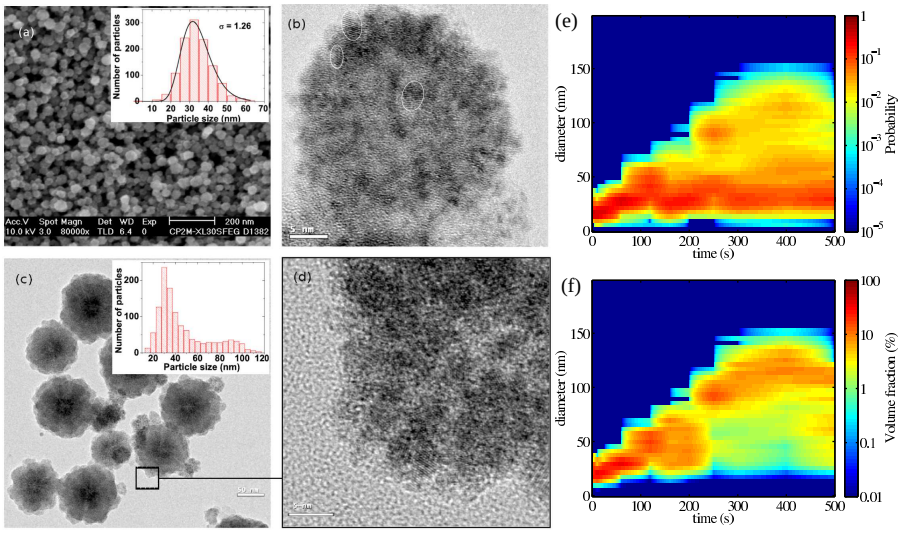

Figure 1: (a) Tungsten dust particles after t= 120 s (SEM). Inset: corresponding size histogram fitted by a log-normal function. (b) HRTEM image of a ∼30 nm PP after t=60 s, which is an agglomerate of nanocrystallites (2-4 nm) (several of these are circled). (c) TEM image of particles after t=300 s. PPs as well as bigger particles (80-120 nm) which appear to be agglomerates of PPs. Inset: the corresponding size histogram build from SEM images. (d) Zoom of the selected edge region of one of the big particles, showing nanocrystallites.(e) Probability to find a particle of given diameter at a given time. (f) Fraction of the total particle volume occupied by particles of a given diameter at a given time.

Evolution of the dust particle size distribution

Representative SEM and TEM images of nanoparticles produced at different plasma durations are shown in Fig.1(a) (t=120 s) and Fig.1(c) (t=300 s). The nanoparticle size histograms are in the inset of Figs. 1(a) and (c). The HR-TEM image of Fig.1(b) shows the structure of a primary particle (PP) of ∼30 nm, produced after 60 s. This PP is made by agglomeration of tungsten crystallites or nanocrystallites of ∼2-4 nm, evidenced by parallel diffraction fringes. These nanocrystallites are the smallest solid units, which are produced but could not be observed separately. For longer discharge durations, the PPs agglomerate to form bigger nanoparticles (80-150 nm) (Fig.1(c)). Examining the edges of such big particles with HR-TEM, PPs as well as the inner nanocrystalites can be observed (Fig.1(d)) A complete evolution of the particle growth during 500s was established from the size distribution measurements. Fig.1(e) shows the

probability (colour-coded) to find a particle of a given size at a given time. Up to ∼120 s, the most probable dust particle diameter was increasing almost linearly from ∼ 15 nm to ∼ 30 nm. Before ∼120 s, the dust particle size distribution could be reasonably fitted with a log-normal distribution. After ∼120 s, two interesting features can be seen: i) ∼30 nm PPs remained the most probable and, ii) big particles were growing in the plasma resulting in the appearance of a second hump in the distribution function as shown in the inset of Fig.1(c). Fig.1(f) presents the evolution of the fraction of the total particle volume (volume fraction, colour-coded) occupied by particles of a given size at a given time. By comparing this figure to Fig.1(e), it can be seen that for discharge duration $\leq$ 120 s, most of the matter was carried by the most probable particle (in size). For longer time, the matter volume of the big particle was steadily increasing and was more prominent than the volume carried by the smaller but more numerous particles.

Evolution of the discharge parameters

In Fig.2, the evolution of the cathode voltage V_d, electron density n_e and line emission intensities are presented and can be divided into four phases named A, B, C and D (Figs.2a-e). Phase A corresponds to the first few seconds after the breakdown. During this phase, the glow appeared to have a uniform intensity under the cathode region (see Fig.2(f)). After the breakdown, the absolute value of the cathode voltage $|V_d|$ decreased in $\simeq$70 ms to $|V_d| \sim$ 500 V and then increased up to $|V_d| \sim$ 650 V in 3-4 s (Fig.2(e)). Meanwhile, the emission intensity of all the lines increased (Fig.2(e)) with a slower growth rate for tungsten lines. The electron density was relatively high just after the breakdown and fell to its lowest measured value towards the end of the phase. At the beginning of Phase B, the cathode voltage dropped by ∼15 V in a time less than 0.5 s and was associated with the simultaneous appearance of a luminous "blue glow" at the center of the tungsten cathode (Fig.2(g)). Then for the next ∼ 30 s, the cathode voltage remained nearly constant. During this time the "blue glow" began to spread towards the edge of the cathode. Towards the end of the phase, V_d started to decrease quickly. OES showed that at the beginning of phase B, all the emission line intensities exhibited a sharp increase (Fig.2(e)) and reached a maximum and started to decrease before the end of the phase. The electron density was continuously increasing throughout this phase. In Phase A and B, the reported evolution correspond to the removal of the oxide layer on tha cathode (tungsten oxide has a better secondary electron emission than pure tungsten at low energy ion bombardment [2] and as the sputtering yield of tungsten is higher than the one of tungsten oxide [3]). The effect of the nanoparticle growth is overcome by the influence of the cathode material. In Phase C, the cathode voltage decreased steadily ($\Delta V_d \sim$150 V) to its lowest value in $\sim 200 - 250$ s. By the end of phase C, the "blue glow" had spread over the cathode

area. OES showed that line intensities of all species continued to decrease (see Fig.2(a-d)). Argon lines reached a minimum towards the end of phase C and the the WII line decreased to noise level. The electron density increased at a faster rate than in phase B and reached a maximum at the end of phase C. During this phase, the modification of the tungsten surface was still playing an important role. However, dust particles were growing in the plasma and the charging phenomena became important. At the end of phase C, dust particles counterbalanced the effect of the modification of the cathode surface. In Phase D, the dust particles, played the main role in the discharge evolution. V_d increased in order to maintain the ionisation as the electron density decreased. Argon line intensities followed V_d likely indicating a rise of the electron temperature. The 656 nm H_α line intensity was also followed in order to monitor the impurity content of the plasma due to the outgasing of the cathode. and indicates that the density of impurities increased during the discharge as expected in experiments without gas flow (constant increase, see Fig.2b).

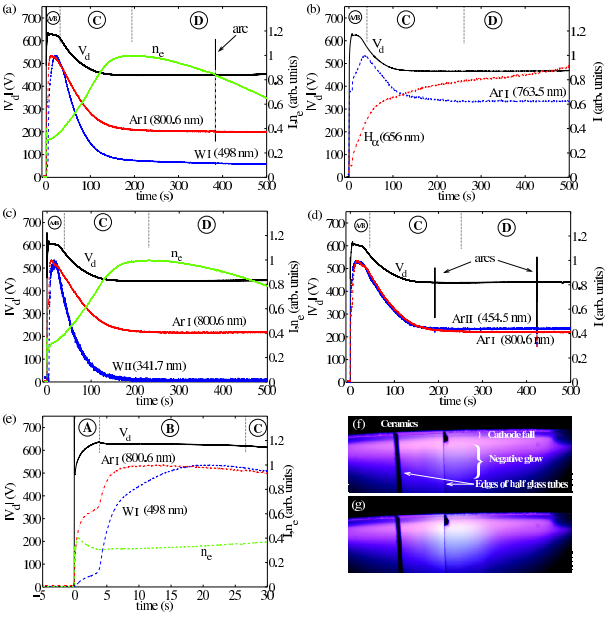

Figure 2: (a-d) Evolutions of the cathode voltage V_d and line intensities as a function of time. The signals are divided in four phases: A, B, C and D. (e) Zoom of (a). (f) Picture of the cathode-fall region and the beginning of the negative glow at the end of phase A. (g) Same as (f) at the start of phase B.

Conclusion

In this article, the growth of tungsten nanoparticles from the sputtering of a tungsten cathode in DC argon glow discharges was investigated. We have shown that the nanoparticles are formed by successive agglomerations. The evolution of the discharge and plasma parameters during particle growth is explained by a competition between the surface state of the tungsten cathode and the influence of the growing nanoparticles.

References

[1] C. Dominique and C. Arnas, J. Appl. Phys. **.101**, 123304 (2007),.

[2] A. V. Phelps and Z. L. Petrovíc, Plasma Sources Sci. Technol. **8**, R21 (1999).

[3] R. Boulmani *et al.*,Sensors and Actuators B: Chemical, **25**, 622 (2007).